Understanding retention and metabolization of aroma compounds using an in vitro model of oral mucosa

Sarah Ployon, Marine Brulé, Isabelle Andriot, Martine Morzel, Francis Canon

Version of Record: https://www.sciencedirect.com/science/article/pii/S0308814620303307
Manuscript_cd7ba2760225ef7c012aee0e7650d9c3

Understanding retention and metabolization of aroma compounds using an *in vitro* model of oral mucosa

*Sarah PLOYON[1], Marine BRULE[1], Isabelle ANDRIOT[1,2], Martine MORZEL[1], Francis CANON[1] **

[1] *Centre des Sciences du Goût et de l'Alimentation, AgroSup Dijon, CNRS, INRAE, Université de Bourgogne Franche-Comté, F-21000 Dijon, France*

[2] *ChemoSens Platform, CSGA, F-21000 Dijon, France*

* Corresponding author: francis.canon@inrae.fr

Abstract

The mechanism leading to aroma persistence during eating is not fully described. This study aims at better understanding the role of the oral mucosa in this phenomenon. Release of 14 volatile compounds from different chemical classes was studied after exposure to *in vitro* models of oral mucosa, at equilibrium by Gas-Chromatography-Flame Ionization Detection (GC-FID) and in dynamic conditions by Proton Transfer Reaction- Mass Spectrometry (PTR-MS). Measurements at equilibrium showed that mucosal hydration reduced the release of only two compounds, pentan-2-one and linalool ($p<0.05$), and suggested that cells could metabolize aroma compounds from different chemical families (penta-2,3-dione, trans-2-hexen-1-al, ethyl hexanoate, nonan- and decan-2-one). Dynamic analyses for pentan-2-one and octan-2-one evidenced that the constituents of the mucosal pellicle influenced release kinetics differently depending on molecule hydrophobicity. This work suggests that mucosal cells can metabolize aroma compounds and that non-covalent interactions occur between aroma compounds and oral mucosa depending on aroma chemical structure.

Keywords

Aroma persistence, oral mucosa, mucosal pellicle, TR146/MUC1 cells, aroma retention, aroma metabolism, aroma release, in vitro model

1. Introduction

When consuming food, most aroma notes are perceived almost instantly after placing food in the mouth and they dissipate rapidly after swallowing, while some continue to be perceived for a longer time. This phenomenon, called aroma persistence or "long lasting aroma" contributes to the quality of food. However, the biological and physicochemical mechanisms responsible for persistence are not fully understood. Aroma perception during eating is a complex process, initiated by the release of odorants from the food into the oral cavity and their transport via the retronasal route to the olfactory receptors in the nose. The main hypothesis for explaining aroma persistence is that aroma compounds adsorb at the surface of the oral mucosa, before being progressively desorbed and released into the oral cavity after the equilibrium has changed due to food swallowing (Buettner, Beer, Hannig, Settles, & Schieberle, 2002; Esteban-Fernãndez, Rocha-Alcubilla, Munoz-Gonzalez, Moreno-Arribas, & Pozo-Bayon, 2016). This implies that aroma compounds bind through non-covalent interactions to the mucosal surface, as reported for tannins in astringency perception (Ployon et al., 2018). Some *in vivo* experiments have evaluated the ability of the oral and pharyngeal mucosae to retain aroma compounds, for example by the Spit-Off Odorant Measurement method, i.e. quantification of odorants remaining in aqueous samples (Buettner et al., 2002; Hussein, Kachikian, & Pidel, 1983) and wine (Esteban-Fernãndez et al., 2016) after expectoration. Other *in vivo* measurements followed in-mouth release of aroma compounds using the Buccal Odor Screening System (Buettner & Welle, 2004) or more recently an intra oral Solid phase Microextraction (SPME) fiber (Esteban-Ferñandez, Munoz-Gonzalez, Jimenez-Giron, Perez-Jimenez, & Pozo-Bayon, 2018; Esteban-Fernãndez et al., 2016) and Proton-Transfer-Reaction Mass Spectrometry (PTR-MS) (Muñoz-Gonzalez, Canon, Feron, Guichard, & Pozo-Bayon, 2019; Sanchez-Lopez, Ziere, Martins, Zimmermann, & Yeretzian, 2016). It emerges from those studies that the physicochemical properties of aroma compounds do not fully explain in-mouth persistence. For example, a decrease of intra-oral persistence with aroma compounds polarity was noted (Buettner & Schieberle, 2000) but guaiacol, a highly polar compound, has high intra-oral retention (Esteban-Fernãndez et al., 2016) and higher persistence than less polar compounds (Muñoz-Gonzalez et al., 2019). Also globally the most persistent compounds are hydrophilic and the least persistent ones are hydrophobic, but there are many exceptions and compounds with similar

hydrophobicity may have very different persistence behaviors (Esteban-Fernãndez et al., 2016; Linforth & Taylor, 2000). This may be explained by the different natures of the non-covalent interactions involved. Another mechanism to consider when studying persistence is that some aromas may be enzymatically converted to new compounds in the oral cavity by salivary enzymes (Buettner, 2002a, 2002b; Pagès-Hélary, Andriot, Guichard, & Canon, 2014) or by cellular enzymes as demonstrated in the nasal cavity (Robert-Hazotte et al., 2019; Schoumacker, Robert-Hazotte, Heydel, Faure, & Le Quere, 2016). The outer part of the oral mucosa is composed of an epithelium onto which is anchored the mucosal pellicle, a hydrated layer of epithelial and salivary proteins (Bradway, Bergey, Jones, & Levine, 1989). Mucins are very abundant at the mucosal surface, specifically the salivary mucins MUC5B and MUC7 (Gibbins, Proctor, Yakubov, Wilson, & Carpenter, 2014). Because mucins have a well-documented capacity to interact with aroma compounds (Friel & Taylor, 2001; Muñoz-González, Feron, & Canon, 2018; Pagès-Hélary et al., 2014; Ployon, Morzel, & Canon, 2017), the involvement of the mucosal pellicle in aroma persistence arouses the interest of food scientists (Canon, Neiers, & Guichard, 2018). The purpose of this work was to evaluate the capacity of the oral mucosa to interact with aroma compounds, to describe the respective role of the cell surface and the mucosal pellicle in this phenomenon and to identify the nature of the interactions involved. The strategy was to measure aroma release in presence of an *in vitro* model of oral mucosa previously developed (Ployon, Belloir, Bonnotte, Lherminier, Canon, & Morzel, 2016). As any simplified model, this system presents some limitations. For example, the preserved cells surface integrity of the model differs from the cell status in the superficial layer of mouth mucosa, and interactions between aromas and other food matrix constituents are not considered. However, the use of an *in vitro* model allowed controlling the experimental parameters (e.g. air flow, volume of the system, pellicle composition) and avoided human inter-individual variability. First, static headspace measurements were performed to investigate the capacity of the model mucosa (without and with a pellicle) to retain aroma compounds at thermodynamic equilibrium, using gas-chromatography – flame ionization detection (GC-FID). Then, a real-time monitoring method by PTR-MS was developed to study the dynamic of aroma compounds release from the model mucosa. The ability of the model mucosa to metabolize aroma compounds was also investigated in both static and dynamic approaches.

2. Material and methods

2.1. Saliva collection

The study was performed in accordance with the guidelines of the declaration of Helsinki. Participants provided written informed consent when enrolling into the study. Saliva was obtained from fifteen volunteers who declared to be in good oral condition. Volunteers refrained from smoking, eating or drinking for at least two hours before saliva collection. Subjects donated saliva during approximately 1 h by spitting out at their own rhythm saliva accumulating spontaneously in their mouth into plastic vessels. Over the whole collection time, plastic vessels were kept on ice in order to limit alteration and bacterial development. All samples were subsequently pooled and centrifuged at 14 000 g for 20 min at 4 °C. The resulting pool of clarified saliva was aliquoted and immediately frozen at – 80 °C.

2.2. Cell-based model of oral mucosa

The TR146/MUC1 cell line was used in this study. Cells were seeded at a density of 4.10^4 cell/cm^2 in 10 ml modified headspace vials coated with Cell-TakTM (Corning Life Sciences, New York, NY, USA). Cells were cultured during 5 days as previously described (Ployon et al., 2016). In order to form a mucosal pellicle, clarified saliva diluted into growth medium (1:1) was deposited onto 5-days cells subcultures for 2 h. After incubation, samples were washed twice with PBS in order to eliminate the non-adsorbed saliva. Exposure to aroma compounds and subsequent analyses were performed immediately after washing with PBS.

2.3. Aroma compounds

Aroma compounds were purchased from Sigma-Aldrich (Saint Quentin Fallavier, France). Compounds used in this study and their relevant chemical properties are listed in table 1. Stock solutions were prepared in water at concentrations below the solubility threshold, and kept at 4°C. In order to evaluate the effect of molecule hydrophobicity, we studied a series of linear methyl ketones from C5 to C10, having a log *P* value, which refers to the molecule hydrophobicity, ranging from 0.91 to 3.73. The effect of the position of the chemical functional group was probed by comparing different methyl ketones having their ketone function in position 2 and 3.

2.4. Toxicity assessment

The toxicity of aroma compounds on TR146/MUC1 cells was evaluated. The cells were seeded in 96-well plates. Confluent cells were incubated with 200 µl of aroma solutions at 10^{-4} mol/l in PBS (except for guaiacol prepared at 10^{-3} mol/l in PBS) for 1 h à 37 °C. The concentrations in mg/l are listed in table 1. Molecule toxicity was assessed using the Neutral Red assay (Rat, Korwinzmijowska, Warnet, & Adolphe, 1994). Briefly, after incubation with aroma compounds, cells were incubated for 3 h at 37 °C with 200 ml of medium containing neutral red at 50 mg/ml, washed twice with PBS and then incubated at room temperature for 1 h in neutral red eluent (ethanol:H_2O:acetic acid, 50:49:1) with gentle agitation. Reading of fluorescence was performed with Victor3V microplate reader (PerkinElmer) with excitation and emission wavelengths fixed at 544 nm and 595 nm, respectively. Assays were performed in duplicates. Viability of cells was above 90% for all aromas, confirming their non-cytotoxicity.

2.5. Evaluation of residual water retained on cell surfaces

After rinsing with PBS, the cells' surface remains covered by a thin layer of residual PBS. Since this residual liquid phase may affect aroma retention and release, the PBS volume remaining onto the cells' surface after rinsing was estimated. Six vials containing the model mucosa were washed with PBS and immediately weighed. Open vials were evaporated for 30 min at room temperature and weighed again. The amount of PBS remaining onto cell surface was estimated as the difference between the two weights and was calculated to be 24.9 ± 5.6 mg. In order to take into account the hydration of mucosa in the experiments, 25 µl of PBS were added to the control vials (without mucosa): this condition is referred to as "hydrated control (HC)".

2.6. Static equilibrium headspace analysis

Single aroma solutions at 10^{-4} mol/l in PBS were prepared from stock solutions (cf table 1), except for guaiacol and pyzarines for which 10^{-3} mol/l solutions were prepared because preliminary work revealed that in our conditions, the molecules were not detected at 10^{-4} mol/l by GC-FID headspace analysis. pH of the solutions was set at 7.4. In order to avoid competition between aroma compounds, each molecule was tested individually. 300 µl of a single aroma solution were added to the vial, which was then sealed with silicone septum in magnetic caps (Supelco, Bellefont, PA, USA).

For each molecule, equilibrium headspace analysis was performed in 4 conditions: an empty vial named dry control (DC), an empty vial with 25 µl of PBS named hydrated control (HC), a vial containing the TR146/MUC1 cells (T) and a vial containing the model mucosa: TR146/MUC1 cells with the mucosal pellicle (TP). Headspace analysis of an empty vial with 25 µl of PBS + 150 µl of clarified saliva + 150 µl of aroma solution at 2.10^4 mol/L (i.e. final concentration of aroma compounds is 10^4 mol/L) (CS) was also performed to determine the effect of the clarified saliva on aroma release. Static headspace sampling (SHS) experiments were performed using GC-FID. Vials were placed into the incubator of an automatic sampler (GERSTEL MPS2, Gerstel Inc., Mülheim an der Ruhr, Germany) and incubated at 37 °C for 40 min. Preliminary experiments confirmed that the thermodynamic equilibrium was reached after this duration in the control condition (HC).

100 µl of the headspace were sampled automatically using a syringe preheated at 42 °C and analyzed in splitless mode by a gas chromatograph coupled to a FID detector (Agilent 7890B, Agilent Technologies, Santa Clara, CA, USA). A 250 µl liner was used. Injector temperature was set at 240 °C and detector temperature was set at 250 °C. A DB-WAX column (30 m, 0.32 mm i.d., 0.5 µm; Agilent Technologies) was used with helium as carrier gas at a velocity of 21 cm/s. For each compound, the oven temperature was set to values leading to a retention time between 2 and 4 min (Table 1). Each condition was tested in triplicate, repeating the analysis sequence DC, HC, T and TP three times. For each aroma compound, a calibration curve was established by GC/FID in the same analytical conditions as reported above and using a 1 µl liquid injection of a solution of aroma compounds in CH_2Cl_2 using OpenLab (Agilent Technologies, Santa Clara, CA, USA) (Supplementary Material S2). The calibration curves were used to determine the concentration of each aroma compound in the gas phase.

2.7. Analysis of compounds degradation by GC-MS.

GC-MS analyses were performed to determine whether bioconversion occurred and to identify the resulting metabolites. The degradation of molecules was tested only for molecules for which a decrease in headspace concentration was observed (i.e pentan-2,3-dione, trans-2-hexen-1-al, ethyl hexanoate, nonan-2-one, and decan-2-one). For those molecules, 5 vials containing the model mucosa without pellicle (T) were incubated 40 min at 37 °C with 300 µl of aroma solution at 10^{-4} mol/l

in PBS. After incubation, supernatants were pooled (i.e. 1.5 ml) and aroma compounds were extracted with 750 µl of CH_2Cl_2. As a control, the same volume of aroma solution (1.5 ml) non exposed to cells was extracted with 750 µl of CH_2Cl_2. 1 µl of extract was analyzed by GC-MS. A 6890A gas chromatograph coupled to a 5973N mass selective detector (Agilent Technologies) was used. For electron ionization (EI), analyses were done at an electron energy of 70 eV at a rate of 4 scans/s, covering the m/z range of 29-350 with a source temperature of 230 °C. The injector temperature was set at 240 °C. A DB-WAX column (30 m, 0.32 mm i.d., 0.5 µm; Agilent Technologies) was used with helium as carrier gas at a velocity of 44 cm/s. The initial oven temperature was set at 40 °C for 5 min then increased to 240 °C at a rate of 5 °C/min. The compounds present in the extract were identified by comparison of their MS spectra to an internal mass spectra database (INRAMASS) and to mass spectra databases (NIST 2008, Wiley 138).

2.8. Conversion rate calculation

For each compound, we determined its concentration in the liquid phase from its partition coefficient in the buffer (HC) and concentration in the gas phase (C_{gas}). First, we calculated the concentration of aroma compounds in the gas phase in the different conditions from the peak areas using the calibration curves (Supp. Material S2). Then, the partition coefficient of each compound was determined in the buffer condition by the formula $K_{HC}= C_{gasHC}/C_{liqHC}$.

Then, the liquid phase concentrations C_{liq} in the T and TP conditions were calculated using the formula $C_{liq(T\ or\ TP)} = C_{gas\ (T\ or\ TP)}/K_{HC}$. Conversion rates were calculated in T or TP condition as following: $r = (C_{liq(T\ or\ TP)}(t0) - C_{liq(T\ or\ TP)}(t40))/ 40$.

2.9. Dynamic aroma release monitoring by PTR-ToF-MS

In this part, two aroma compounds that did not appear metabolized by the cells were tested: pentan-2-one (MH^+ m/z = 87.14) and octan-2-one (MH^+ m/z = 129.22). Aroma solutions at 10^{-5} mol/l in PBS ([pentan-2one] = 0.86 mg/l and [octan-2-one] = 1.28 mg/l) were prepared from stock solutions. 300 µl were injected in the vial using an automatic liquid dropper. Three biological replicates were analyzed per aroma compound. Compounds were analyzed separately in order to avoid competition using proton transfer reaction – mass spectrometry (PTR-MS). This technique allows the ionization of a volatile molecule through a proton transfer from $[H_2O+H]^+$ ions to the volatile depending on its proton

affinity. For most volatile organic compounds their proton affinity is above that of water. The instrument used in this study includes a time-of-flight analyzer providing high resolution and high speed of acquisition. Thus, this instrument allows real time monitoring on a large range of m/z of volatile organic compounds, such as aromas. Furthermore, this more sensitive technique allows using lower aroma concentrations: this presents the advantage of limiting the risk of saturating the mucosa. The experimental device is illustrated in figure 4A. A PTR-ToF-MS (PTR-ToF-MS 8000, Ionicon Analytik, Innsbruck, Austria) was used with a scanning speed of 108 ms/spectrum for a mass range from 0 to 250 u. Calibration was performed following ions at m/z 21.022086 u ($[H_2{}^{18}O + H]^+$); 39.03265 u $[H_2O{\bullet}H_2{}^{18}O + H]^+$ and 59.042141 [acetone + H]$^+$. $[H_2O + H]^+$ was used as reacting ion. Analyses were performed under a drift tube pressure of 2.3 mbar, at 80 °C, a voltage of 490 V and a ratio E/N of 110 Td. The air flow at the entrance of the system was set at 100 ml/min.

A vial containing the model mucosa, without (T) or with (TP) a mucosal pellicle, was closed by a 3-way cap with silicon septum. A first way was connected to a Tedlar® bag containing wet air. A second way was connected to the PTR-MS. Aroma injection was performed through the third way. Two 3-way automatic valves were used to direct the airflow way through to two parallel circuits. The circuit connected to the glass vial with the model mucosa is called “indirect”, while the second circuit, directly connected to the Tedlar® bag, is called “direct”. The experiment started with the circuit in direct position. Aromatized gas was injected into the vials by the third way of the vial cap and exposed to the model mucosa for 1 min. Then, the circuit was turned to the indirect position and the air flow from the Tedlar® bag swept the glass vial headspace to the PTR for 3 minutes. The composition of the gas was analyzed by PTR-MS analysis. Area under the curve of the ions $[C_5H_8O+H]^+$ (m/z = 87.14) and $[C_8H_{16}O+H]^+$ (m/z = 129.22) were extracted from the mass spectra as a function of time (Supplementary Material S1a). Then the average noise signal during the first 60 sec of acquisition was subtracted. The resulting curves of each of the peak area of the two ions as a function of time were established (Supplementary Material S1b). From these curves, the maximum intensity (Imax) and cumulated area (CA) as a function of time were determined for each condition (Supplementary Material S1c). Data were extracted using IgorPro 6.36 (Igor Pro Wavemetrics, USA).

2.10. Statistical analysis

For each aroma compound, partition coefficients measured by GC-FID in the DC and in the HC conditions (i.e. K_{DC} and K_{HC}), and in the HC and the CS (ie K_{HC} and K_{CS}) were compared using a Student t-test (alpha = 0.05). HC was used as control for all further experiments. Partition coefficients measured in the different conditions (i.e. K_{HC}, K_T or K_{TP}) were submitted to univariate analysis of variance (ANOVA) followed by a Tukey multiple comparison test (significance for $p<0.05$).

Aroma conversion rates calculated in the T and in the TP conditions were compared using a Student t-test (alpha = 0.05). Conversion rates of all aroma compounds for each condition (T or TP) were submitted to univariate analysis of variance (ANOVA) followed by a Tukey multiple comparison test (significance for $p<0.05$).

For PTR-MS analysis, Imax and CA in the three conditions HC, T or TP were compared by ANOVA followed by a post-hoc Tukey multiple comparison test (significance for $p<0.05$).

3. Results and discussion

3.1. Effect of mucosal hydration on aroma partitioning

The mucosal pellicle is a lubricating layer containing mucins anchored at the surface of the epithelial cells. Mucins have hydrophilic regions with the ability to form H-bonds and electrostatic interactions (Bansil & Turner, 2006). As a consequence, the mucosal surface is wet and this property has to be considered as a factor that impacts on aroma retention (Déléris, Saint-Eve, Saglio, Souchon, & Trelea, 2016). As described in the materials and methods section, we determined that the surface of the model mucosa retains on average 24.9 ± 5.6 mg of buffer. In order to evaluate how this surface wetness impacts aroma partitioning, the partition coefficients (K) in the dry control (DC) and hydrated control (HC) conditions were measured and the ratio between the two partition coefficients was calculated for each studied molecule (figure 1A). A ratio below 100 % indicates that the considered aroma compound is significantly retained by the residual liquid. The signal/noise ratios for pyrazine and 2'3-dimethylpyrazine were below the limit of quantification, therefore it was not possible to establish the impact of the cells' wetness on their release. For the other compounds, we observed that the residual buffer significantly retained pentan-2-one (-18 ± 7 %) ($p<0.05$) of the 2-methyl ketone series, while hexan-2-one (-19 ± 3 %), and octan-2-one (-10 ± 4 %), heptan-2-one (-8 ± 5 %), nonan-2-one (-6 ± 7 %) and decan-2-one (-5 ± 9 %) were also retained but not significantly. Regarding other compounds, they tended to be retained by the presence of the buffer (except guaiacol), however this effect was only significant for linalool ($p<0.05$). This global tendency, despite being significant only for pentan-2-one and linalool, suggests that a part of aroma compounds is transferred into the buffer according to the thermodynamic laws and to their affinity for the liquid phase, decreasing the amount of aroma in the headspace. This could for example explain the high persistence of hydrophilic compounds such as pyrazines (Buffo, Rapp, Krick, & Reineccius, 2005; Linforth et al., 2000; Wright, Hills, Hollowood, Linforth, & Taylor, 2003) or small alcohols (ethanol, propan-2-ol) previously observed (Linforth et al., 2000).

Since the presence of residual buffer on cells surface affected the partitioning of several compounds, the HC condition was used in the rest of the study as a control to test the effect of the cells and the mucosal pellicle.

3.2. Aroma partitioning in presence of oral cells and/or a mucosal pellicle

Partition coefficients (K) were measured by static headspace analyses (SHS) in the hydrated control (HC), TR146/MUC1 (T) and TR146/MUC1 + mucosal pellicle (TP) conditions after 40 min of incubation at 37 °C. Results are presented in figure 1B, as the ratio between the K values in the condition T or TP (K_T or K_{TP}) and the partition coefficient in the control HC (K_{HC}). A ratio lower than 100% indicates that aroma release is lower in the vial containing the cells alone (T) or the model mucosa with a mucosa pellicle (TP) than in the control vial (HC).

The partitioning ratios calculated for hexan-3-one, guaiacol, octan-3-one and the four other linear ketones pentan-2-one, hexan-2-one, heptan-2-one and octan-2-one indicate that there were no significant differences in the K_T and K_{TP} of these compounds compared to the K_{HC} (control condition). Thus, the release of these compounds was not affected by the model mucosa with and without pellicle at equilibrium.

In contrast, a significant decrease ($p<0.05$) of aroma partitioning was observed in both conditions T and TP compared to the HC control condition, for pentan-2,3-dione (-73 ± 16 %, for T and - 83 ± 1 % for TP), trans-2-hexen-1-al (-69 ± 3 % for T and - 75 ± 1 % for TP), ethyl hexanoate (-16 ± 3 % for T and - 19 ± 6 % for TP), nonan-2-one (-16 ± 3 % for T and - 17 ± 3 % for TP) and decan-2-one (-37 ± 6 % for T and - 34 ± 6 % for TP). There was no significant difference measured between the conditions with and without pellicle, except for trans-2-hexen-1-al, which was significantly less released in presence of the mucosal pellicle. The effect of diluted clarified saliva on the partition coefficient of these aroma compounds was also measured by SHS: there was no retention effect of saliva (CS) compared to the control condition of aroma diluted in the buffer without saliva (HC) (figure 1C). Interestingly, even though a strong effect of the model oral mucosa was observed on penta-2,3-dione partitioning, it did not impact the partitioning of the mono ketone pentan-2-one. The position of the ketone group on hexan-2 or 3-one and octan-2 or 3-one (i.e. in C2 or C3) did not modify the effect of the model mucosa.

Aroma compounds exhibit a large range of hydrophobicity. This physico-chemical characteristic can be at the origin of their behavior. The hydrophobicity of a molecule can be measured by determining its octanol/water partition coefficient, abbreviated log *P*. The higher log *P* value of a compound, the higher the compound's hydrophobicity.

Ketones belonging to the 2-methyl ketone series differ only by the length of their aliphatic chain, which is correlated to the molecule hydrophobicity. Thus, in order to probe the effect of molecule hydrophobicity, the ratios K_T/K_{HC} and K_{TP}/K_{HC} were expressed as a function of log *P* values (figures 2A and 2B). Partitioning of molecules when exposed to the model mucosa appeared to be negatively correlated with log *P* (R^2 = 0.87 and R^2= 0.96 respectively for T and TP), meaning that molecules were less readily released from the model mucosa as their hydrophobicity increased. A negative correlation between linear methyl ketones partitioning in presence of salivary proteins and molecules hydrophobicity was previously reported (Pagès-Hélary et al., 2014). Here, the slopes of the curves were comparable (-0.161 and -0.167 respectively for T and TP), indicating that there is no effect of the pellicle on the partitioning of methyl ketones for cells expressing MUC1 at their surface. When plotting K values of the 13 molecules as function of their log *P*, no correlation was found between molecule hydrophobicity and retention by the oral mucosa (R = 0.09, data not shown). The two compounds for which partitioning was the most reduced in the presence of the model mucosa, pent-2,3-dione (log *P* = -0.85) and trans-2-hexen-1-al (log *P* = 1.58), have very different hydrophobicity. Therefore, it appears that the functional group has also a strong impact on the effect of the model mucosa on aroma release.

In order to explain the effect of the model mucosa on aroma release, two main hypotheses can be formulated. The first one is that aromas bind to the surface of the cells in presence or not of the mucosal pellicle. The second one postulates that the cell line is able to metabolize the studied aroma compounds.

3.3. Compounds degradation by model mucosa

In order to explore the hypothesis that modification of the release of aroma compounds in presence of the model of oral mucosa results from their metabolization by cells, the composition of the liquid phase of aroma solutions incubated in presence of the model mucosa without pellicle was characterized by GC–MS after extraction with dichloromethane for pentan-2,3-dione, trans-2-hexen-1-al, ethyl hexanoate, nonan-2-one and decan-2-one. The example of nonan-2-one extracts analyses is presented in figure 3. A decrease in the initial concentration of nonan-2-one (eluted at 13.1 min) was observed in the same order of magnitude of the one observed in GC-FID. A new

319 compound eluted at 16.5 min (figure 3B) in the presence of cells compared to the hydrated control
320 extract (figure 3A). MS spectrum extracted at 16.5 min is provided in figure 3C. Comparison with MS
321 databases allowed identifying the new compound as nonan-2-ol. The chromatograms and MS
322 spectra of the five compounds studied are given in supplementary material S3. For the five aroma
323 compounds, a decrease in initial compounds amount in comparison to the control condition was
324 associated with the presence of new compounds in the T condition. The identified molecules and
325 the conversion rate of initial compounds in the T and TP conditions are reported in table 2. The
326 decrease in nonan-2-one and decan-2-one concentrations was associated with the production of the
327 corresponding alcohols, namely nonan-2-ol and decan-2-ol, respectively. Decrease of pentan-2,3-
328 dione solution concentration was associated with the production of two reduced forms of the
329 molecule: 2-hydroxy-pentan-3-one and 3-hydroxy-pentan-2-one. Ethyl hexanoate was hydrolyzed
330 into hexanoic acid, and trans-2-hexen-1-al was oxidized into its corresponding acid hexenoic acid.

331 Although conversion rates of aroma by the model mucosa were in the same order of magnitude,
332 small differences were observed between aroma compounds. Pentan-2,3-dione and trans-2-hexen-
333 1-al were converted significantly ($p<0.05$) faster. Concerning the impact of the mucosal pellicle, a
334 significant difference between the oral mucosa with and without the mucosal pellicle was observed
335 only for trans-2-hexen-1-al. These observations indicate that the TR146/MUC1 cell line is able to
336 metabolize the molecules reported in table 2. The ability of epithelial cells to metabolize organic
337 volatile compounds from different chemical families has already been observed on primary cells
338 cultures of human nasal mucosa or rat olfactory mucosa. Zaccone et al (2015) reported oxidation of
339 two diketones into monoketones (diacetyl and pentan-2,3-dione to 3-hydroxybutanone and 2-
340 hydroxy-3-pentanone, respectively) in a culture of bronchial/tracheal human epithelial cells (Zaccone
341 et al., 2015). Microsomal and cellular fractions obtained from rat olfactory mucosa exhibited ability
342 to metabolize quinoline (heterocycle) and coumarin (lactone) into oxygenated metabolites, and
343 isoamyl acetate (ester) into isoamylic alcohol (Thiebaud et al., 2013). Although the respective
344 contributions of the mucus and the epithelial cells was not determined, *ex vivo* rat olfactory mucosa
345 converted ethyl acetate into ethanol (Schoumacker et al., 2016) and pentan-2,3-dione into 2-
346 hydroxy-pentan-3-one and 3-hydroxy-pentan-2-one (Robert-Hazotte et al., 2019). These reactions

347 are catalyzed by a range of enzymes named Odorant Metabolizing Enzyme (OME) (Heydel, Hanser,
348 Faure, & Neiers, 2017) that belong to the xenobiotic metabolism enzymes (XMEs) family. Overall,
349 XMEs are specialized in the catabolism of exogenous compounds in order to facilitate their
350 elimination by the organism (Croom, 2012). Xenobiotics elimination results from three mains steps.
351 During the first phase, nonpolar and reactive compounds are converted into more polar and less
352 reactive compounds through different reactions, such as epoxidation, hydroxylation, desalkylation,
353 oxidation or reduction. This step involves enzymes such as the cytochrome P450 or
354 carboxylesterase (Thiebaud et al., 2013). In the second phase, conjugate enzymes, such as
355 glutathione transferase, catalyze reaction of conjugation with polar compound such as glutathione,
356 glucuronic acid or a sulfate (Heydel et al., 2019). Finally, metabolites can be easily excreted via
357 transporter proteins. The OMEs family includes a large variety of enzymes. The reduction of pentan-
358 2,3-dione into 2-hydroxy-pentan-3-one and 3-hydroxy-pentan-2-one, previously observed in
359 presence of bronchial/tracheal human epithelial cells and rat nasal mucosa has been attributed to
360 the dicarbonyl/L-xylulose reductase (DCXR) (Robert-Hazotte et al., 2019; Zaccone et al., 2015).
361 Hydrolysis of isoamyle acetate into its corresponding acid has been previously attributed to a
362 carboxylesterase (Thiebaud et al., 2013). Thus, we hypothesized that the conversion of ethyl
363 hexanoate into acid hexanoic is catalyzed by a carboxylesterase. Regarding the conversion of
364 ketones into alcohols, such activity has been previously reported in presence of saliva and was
365 proposed to be due to an aldo-keto reductase (Muñoz-González, Feron, Brulé, & Canon, 2018). The
366 oxidation of aldehyde (Trans-2-hexen-1-al) into carboxylic acid (hexenoic acid) could result from the
367 activity of aldehyde dehydrogenases. Moreover, the presence of aldo-keto reductases (AKR1C3,
368 AKR1C2, AKR7AC2, AKR1C1, SPR and KCNAB2) DCXR, carboxylestease (CES1, CES2, CES3,
369 CES4A) and aldehyde dehydrogenases (ALDH9A1, ALDH1B1, ALDH3A1, ALDH3B2, ALDH4A1,
370 ALDH5A1, AGPS) in the oral mucosa has been previously reported using specific antibodies (Uhlén
371 et al., 2015). All these enzymes have been reported to be present in the oral mucosa at different
372 concentrations (Uhlén et al., 2015), which could explain the difference of metabolization between
373 the different affected compounds. RNA encoding for cytochrome P450 have been detected in
374 salivary glands (Kragelund et al., 2008) and human oral mucosa (Vondracek et al., 2001).
375 Carboxylesterase activity has already been observed in rats and mice's oral cavity (Robinson,

376 Bogdanffy, & Reed, 2002). The presence of these enzymes in the oral mucosa indicates that this
377 latter has the potential to metabolize xenobiotics. Indeed, like the nasal cavity, oral mucosa is a
378 tissue exposed to exogenous and potentially toxic compounds, which have to be eliminated. From a
379 sensory point of view, it was recently reported that metabolic activity in the nasal and oral cavities
380 impacts on perception (Ijichi et al., 2019). This work demonstrates for the first time the importance
381 of aroma conversion activity in oral mucosal cells. This activity is probably due to different enzymes,
382 which have different enzymatic activities (kinetics, affinity,…) on aroma compounds as a function of
383 their structure.

384 ### 3.4. Effect of oral mucosa on kinetics of *in vitro* aroma release

385 In-mouth aroma release is a dynamic process. Static headspace (SHS) experiments require the
386 establishment of the thermodynamic equilibrium, which takes approximatively 20 min (Pagès-Hélary
387 et al., 2014). To obtain information on earlier phases, we studied the kinetic release of two aroma
388 compounds unaffected by the presence of the epithelial cells, pentan-2-one and octan-2-one, during
389 the first 2.5 minutes using Proton-Transfer-Reaction Mass Spectrometry (PTR-MS).
390 The maximum of intensity (Imax) and the cumulated area (CA) of aroma release at t= 5, 15, 30, 60,
391 90, 120 and 160 sec in the 2 conditions T and TP are presented in figure 4.
392 There was no significant difference in the Imax for octan-2-one between the three conditions , i.e. in
393 buffer (HC) or in presence of the model mucosa with (TP) and without pellicle (T). However, for
394 pentan-2-one the Imax was significantly higher in presence of the cells with the mucosal pellicle (TP
395 vs HC), but was not significantly different between T and TP conditions. This observation suggests
396 that the rate of transfer of molecules pentan-2-one from the gas phase to the liquid phase is affected
397 by the presence of cells plus the mucosal pellicle. The cells could indeed alter the capacity of water
398 to solubilize the molecules and provoke a salting-out effect explaining the increase of the intensity
399 of the release in presence of the cells plus the mucosal pellicle for pentan-3-one. The absence of
400 effect for octan-2-one could be explain by non-covalent interactions between the compound and the
401 cells with or without the mucosal pellicle, decreasing the result of this salting-out effect.

402 For pentan-2-one, a significant decrease in cumulated area values was observed for all times after
403 60 sec for the TP conditions. Furthermore, a significant difference was measured between the two

404 conditions at 160 sec, with a significantly lower release from the model with a mucosal pellicle
405 compared to the cells-only model (figure 4C). In other words, the reduced release was observable
406 more rapidly when cells were lined by a mucosal pellicle.
407 Regarding octan-2-one release, a significant decrease of octan-2-one release occurred after 120
408 sec for the condition T compared to the control condition (figure 4D). Thus, the reduced release was
409 greater for cells with the mucosal pellicle for pentan-2-one, while it was greater for cells without the
410 salivary proteins forming the pellicle for octan-2-one. In these experiments, we used the
411 TR146/MUC1 cell line which expresses at its surface the extracellular domain of the mucin MUC1/Y-
412 LSP (Zhang, Vlad, Milcarek, & Finn, 2013). The presence of this domain at the cells' surface
413 increases the anchoring of the salivary proteins (Ployon et al., 2016), while modifying the cell surface
414 properties. Atomic Force Microscopy (AFM) experiments using functionalized tip and conducted on
415 the TR146/MUC1 cell line revealed first that the surface of the cells present both highly hydrophobic
416 and hydrophilic domains due to the expression of MUC1/Y-LSP, and second that the anchoring of
417 salivary proteins decreases the number of these highly hydrophobic or hydrophilic domains,
418 suggesting that the anchoring of salivary proteins involves these domains (Aybeke et al., 2019).
419 Thus, the surface of the model mucosa is less hydrophobic in presence of the mucosal pellicle (TP)
420 than without it (T). Octan-2-one differs from pentan-2-one by the length of the aliphatic chain making
421 this molecule more hydrophobic. Previous investigations on the effect of mucin on aroma release
422 have revealed that mucin can retain aroma compounds through non-covalent interactions involving
423 hydrophobic effect (Pagès-Hélary et al., 2014). Therefore, it can be hypothesized that the most
424 hydrophobic compounds are more prone to interact with the most hydrophobic cell surface (cells
425 without a mucosal pellicle T), which is the case for octan-2-one. Conversely, pentan-2-one, which is
426 less hydrophobic, is significant more retained in presence of the salivary proteins forming the
427 mucosal pellicle. This result suggests that pentan-2-one is more prone to interact with salivary
428 proteins than octan-2-one. This observation could be explained by the hypothesis that the presence
429 of salivary proteins increases the number of pentan-2-one binding sites, while the longer aliphatic
430 chain of octan-2-one precludes its access to these binding sites due to steric hindrance. The nature
431 of the non-covalent interaction involved remains unknown.
432 To summarize, the anchoring of salivary proteins to MUC1 changes the cell surface properties and

433 the nature of the exposed aroma binding sites. As a result, it modifies the ability of the mucosa to
434 interact with aroma compounds depending on their structure, leading to either a decrease or an
435 increase of the binding of some aroma compounds and to a modification of the release of aroma
436 compounds through time depending on their structure. The present study suggests that both
437 compounds are less released in presence of the epithelial cells both with or without the mucosal
438 pellicle. Moreover, this latter decreases the release of pent-2-one while it does not significantly affect
439 octan-2-one. As a result, the mucosal pellicle seems to play a role in aroma persistence as a function
440 of aroma compounds structure.

4. Conclusion

The study allowed deciphering the respective impact of hydration, the epithelial cells and the mucosal proteins on the release of several aroma compounds. First, hydration of the mucosal surface modified the release of only two aroma compounds over 13 studied (here, pentan-2-one and linalool), suggesting that it does not play a prominent role in the impact of the oral mucosa on aroma release.

The model mucosa impacted both the partitioning of pentan-2,3-dione, trans-2-hexen-1-al, ethyl hexanoate, nonan-2-one and decan-2-one at equilibrium and the release of the pentan-2-one and octan-2-one (the only two aroma compounds studied in dynamic condition). This impact appears to result from the ability of oral cells to metabolize aroma compounds (herein methyl ketones, aldehydes and esters) depending on their structure. The ability of cells to metabolize aroma compounds results from the activity of the enzymes that they express. Enzymes are biological catalysts that accelerate specific chemical reactions as a function of their three-dimensional structure and the structure of the metabolized compound. OMEs which specifically metabolize different families of aroma compounds, are present in the oral mucosa at different concentrations to detoxify reactive aroma compounds as a function of their structure. The metabolic activity observed here could result from the activity of DCXR for pentan-2,3-dione, aldo-keto-reductases for nonan-2-one and decan-2-one, carboxyesterase for ethyl hexanoate and aldehyde dehydrogenase for trans-2-hexen-1-al. Moreover, the difference of activity observed between the different compounds could result from either a difference in the enzymatic reaction as a function of the affinity of the enzyme – aroma compound couple and/or differences of enzyme concentrations as previously reported in the oral mucosa. Thus, no generalization could be drawn and each compound is a specific case that will be metabolized as a function of its structure and the composition of the oral epithelial cell proteome. The dynamic study was only performed on two compounds (here two 2-methyl ketones) and suggested that other phenomena such as non-covalent interactions between the two studied aroma compounds and mucosa (cells and mucosal pellicle) also occur. As a result, times after 60 s were significantly affected for both molecules, with a decrease of their release in presence of the cells and the pellicle mucosal. The mucosal pellicle significantly affected the release of pentan-2-one in the

469 TR146/MUC1/Y-LSP cell line. Thus, this model of mucosa appears as a promising tool to study the
470 effect of the oral mucosa on aroma release as a function of aroma compounds structure and/or
471 pellicle composition. It may also aid in further researches on the role of the mucosa on aroma
472 metabolization. In the future, it would be of interest to perform real time monitoring of aroma release
473 and persistence in nasal and/or oral cavities after *in vivo* consumption of aroma solution in order to
474 establish a comparison with *in vitro* experiments.
475 To conclude, this paper, by demonstrating that the oral mucosa both impacts the kinetic of aroma
476 compounds release and metabolizes aroma compounds, opens new avenues of research on the
477 role of the oral mucosa in aroma persistence and aroma perception.

Conflict of interest statement

The authors declare no conflict of interest.

Acknowledgments

This work was funded by the French National Research Agency (MUFFIN N° 14-CE20-0001-01). The French Ministry of Higher Education and Research provided the PhD fellowship for Sarah Ployon.

The authors thank the ChemoSens Platform, especially Etienne Semon, for analytical support.

References

Aybeke, E. N., Ployon, S., Brulé, M., De Fonseca, B., Bourillot, E., Morzel, M., . . . Canon, F. (2019). Nanoscale Mapping of the Physical Surface Properties of Human Buccal Cells and Changes Induced by Saliva. *LANGMUIR, 35*(39), 12647-12655. https://doi.org/10.1021/acs.langmuir.9b01979.

Bansil, R., & Turner, B. S. (2006). Mucin structure, aggregation, physiological functions and biomedical applications. *Current Opinion in Colloid & Interface Science, 11*(2–3), 164-170. https://doi.org/10.1016/j.cocis.2005.11.001.

Bradway, S. D., Bergey, E. J., Jones, P. C., & Levine, M. J. (1989). Oral mucosal pellicle - adsoprtion and transpeptidation of salivary components to buccal epithelial-cells. *Biochemical Journal, 261*(3), 887-896. https://doi.org/10.1042/bj2610887.

Buettner, A. (2002a). Influence of human saliva on odorant concentrations. 2. aldehydes, alcohols, 3-Alkyl-2-methoxypyrazines, methoxyphenols, and 3-hydroxy-4,5-dimethyl-2(5H)-furanone. *Journal of Agricultural and Food Chemistry, 50*(24), 7105-7110. https://doi.org/10.1021/jf020714o.

Buettner, A. (2002b). Influence of human salivary enzymes on odorant concentration changes occurring in vivo. 1. Esters and thiols. *Journal of Agricultural and Food Chemistry, 50*(11), 3283-3289. https://doi.org/10.1021/jf011586r.

Buettner, A., Beer, A., Hannig, C., Settles, M., & Schieberle, P. (2002). Quantitation of the In-Mouth Release of Heteroatomic Odorants. In *Heteroatomic Aroma Compounds* (pp. 296-311): American Chemical Society.

Buettner, A., & Schieberle, P. (2000). Influence of mastication on the concentrations of aroma volatiles — some aspects of flavour release and flavour perception. *Food Chemistry, 71*(3), 347-354. https://doi.org/10.1016/S0308-8146(00)00199-0.

Buettner, A., & Welle, F. (2004). Intra-oral detection of potent odorants using a modified stir-bar sorptive extraction system in combination with HRGC-0 known as the buccal odor screening system (BOSS). *Flavour and Fragrance Journal, 19*(6), 505-514. https://doi.org/10.1002/ffj.1473.

Buffo, R. A., Rapp, J. A., Krick, T., & Reineccius, G. A. (2005). Persistence of aroma compounds in human breath after consuming an aqueous model aroma mixture. *Food Chemistry, 89*(1), 103-108. https://doi.org/10.1016/j.foodchem.2004.02.038.

Canon, F., Neiers, F., & Guichard, E. (2018). Saliva and Flavor Perception: Perspectives. *Journal of Agricultural and Food Chemistry, 66*(30), 7873-7879. https://doi.org/10.1021/acs.jafc.8b01998.

Croom, E. (2012). Metabolism of Xenobiotics of Human Environments. *Toxicology and Human Environments, 112*, 31-88. https://doi.org/10.1016/B978-0-12-415813-9.00003-9.

Déléris, I., Saint-Eve, A., Saglio, A., Souchon, I., & Trelea, I. C. (2016). Insights in aroma compound retention by mucosa during consumption through mathematical modelling. *Journal of Food Engineering, 190*, 123-138. https://doi.org/10.1016/j.jfoodeng.2016.06.018.

Esteban-Ferñandez, A., Munoz-Gonzalez, C., Jimenez-Giron, A., Perez-Jimenez, M., & Pozo-Bayon, M. A. (2018). Aroma release in the oral cavity after wine intake is influenced by wine matrix composition. *Food Chemistry, 243*, 125-133. https://doi.org/10.1016/j.foodchem.2017.09.101.

Esteban-Fernãndez, A., Rocha-Alcubilla, N., Munoz-Gonzalez, C., Moreno-Arribas, M. V., & Pozo-Bayon, M. A. (2016). Intra-oral adsorption and release of aroma compounds following in-mouth wine exposure. *Food Chemistry, 205*, 280-288. https://doi.org/10.1016/j.foodchem.2016.03.030.

Friel, E. N., & Taylor, A. J. (2001). Effect of Salivary Components on Volatile Partitioning from Solutions. *Journal of Agricultural and Food Chemistry, 49*(8), 3898-3905. https://doi.org/10.1021/jf010371e.

Gibbins, H. L., Proctor, G. B., Yakubov, G. E., Wilson, S., & Carpenter, G. H. (2014). Concentration of salivary protective proteins within the bound oral mucosal pellicle. *Oral Diseases, 20*(7), 707-713. https://doi.org/10.1111/odi.12194.

Heydel, J.-M., Menetrier, F., Belloir, C., Canon, F., Faure, P., Lirussi, F., . . . Neiers, F. (2019). Characterization of rat glutathione transferases in olfactory epithelium and mucus. *PLoS ONE, 14*(7), e0220259. https://doi.org/10.1371/journal.pone.0220259.

Heydel, J. M., Hanser, H. I., Faure, P., & Neiers, F. (2017). Odorant metabolizing enzymes in the peripheral olfactory process. *Flavour: From Food to Perception*, 34-56. https://doi.org/Book_Doi 10.1002/9781118929384.

Hussein, M. M., Kachikian, R., & Pidel, A. R. (1983). Analysis for Flavor Residuals in the Mouth by Gas Chromatography. *Journal of Food Science, 48*(6), 1884-1885. https://doi.org/10.1111/j.1365-2621.1983.tb05113.x.

Ijichi, C., Wakabayashi, H., Sugiyama, S., Ihara, Y., Nogi, Y., Nagashima, A., . . . Touhara, K. (2019). Metabolism of Odorant Molecules in Human Nasal/Oral Cavity Affects the Odorant Perception. *Chemical Senses*. https://doi.org/10.1093/chemse/bjz041.

Kragelund, C., Hansen, C., Torpet, L. A., Nauntofte, B., Brosen, K., Pedersen, A. M. L., . . . Reibel, J. (2008). Expression of two drug-metabolizing cytochrome P450-enzymes in human salivary glands. *Oral Diseases, 14*(6), 533-540. https://doi.org/10.1111/j.1601-0825.2007.01415.x.

Linforth, R., & Taylor, A. J. (2000). Persistence of volatile compounds in the breath after their consumption in aqueous solutions. *Journal of Agricultural and Food Chemistry, 48*(11), 5419-5423. https://doi.org/10.1021/jf000488n.

Muñoz-Gonzalez, C., Canon, F., Feron, G., Guichard, E., & Pozo-Bayon, M. A. (2019). Assessment Wine Aroma Persistence by Using an in Vivo PTR-ToF-MS Approach and Its Relationship with Salivary Parameters. *Molecules, 24*(7). https://doi.org/10.3390/molecules24071277.

Muñoz-González, C., Feron, G., Brulé, M., & Canon, F. (2018). Understanding the release and metabolism of aroma compounds using micro-volume saliva samples by ex vivo approaches. *Food Chemistry, 240*, 275-285. https://doi.org/10.1016/j.foodchem.2017.07.060.

Muñoz-González, C., Feron, G., & Canon, F. (2018). Main effects of human saliva on flavour perception and the potential contribution to food consumption. *Proceedings of the Nutrition Society*, 1-9. https://doi.org/10.1017/S0029665118000113.

Pagès-Hélary, S., Andriot, I., Guichard, E., & Canon, F. (2014). Retention effect of human saliva on aroma release and respective contribution of salivary mucin and α-amylase. *Food Research International, 64*, 424-431. https://doi.org/10.1016/j.foodres.2014.07.013.

Ployon, S., Belloir, C., Bonnotte, A., Lherminier, J., Canon, F., & Morzel, M. (2016). The membrane-associated MUC1 improves adhesion of salivary MUC5B on buccal cells. Application to development of an in vitro cellular model of oral epithelium. *Archives of Oral Biology, 61*, 149-155. https://doi.org/10.1016/j.archoralbio.2015.11.002.

Ployon, S., Morzel, M., Belloir, C., Bonnotte, A., Bourillot, E., Briand, L., . . . Canon, F. (2018). Mechanisms of astringency: Structural alteration of the oral mucosal pellicle by dietary tannins and protective effect of bPRPs. *Food Chemistry, 253*, 79-87. https://doi.org/10.1016/j.foodchem.2018.01.141.

Ployon, S., Morzel, M., & Canon, F. (2017). The role of saliva in aroma release and perception. *Food Chemistry, 226*, 212-220. https://doi.org/10.1016/j.foodchem.2017.01.055.

Rat, P., Korwinzmijowska, C., Warnet, J. M., & Adolphe, M. (1994). New in-Vitro Fluorometric Microtitration Assays for Toxicological Screening of Drugs. *Cell Biology and Toxicology, 10*(5-6), 329-337. https://doi.org/10.1007/Bf00755779.

Robert-Hazotte, A., Schoumacker, R., Semon, E., Briand, L., Guichard, E., Le Quere, J. L., . . . Heydel, J. M. (2019). Ex vivo real-time monitoring of volatile metabolites resulting from nasal odorant metabolism. *Sci Rep, 9*(1), 2492. https://doi.org/10.1038/s41598-019-39404-x.

Robinson, D. A., Bogdanffy, M. S., & Reed, C. J. (2002). Histochemical localisation of carboxylesterase activity in rat and mouse oral cavity mucosa. *Toxicology, 180*(3), 209-220. https://doi.org/10.1016/S0300-483x(02)00375-X.

Sanchez-Lopez, J. A., Ziere, A., Martins, S. I. F. S., Zimmermann, R., & Yeretzian, C. (2016). Persistence of aroma volatiles in the oral and nasal cavities: real-time monitoring of decay rate in air exhaled through the nose and mouth. *Journal of Breath Research, 10*(3). https://doi.org/Artn 03600510.1088/1752-7155/10/3/036005.

Schoumacker, R., Robert-Hazotte, A., Heydel, J. M., Faure, P., & Le Quere, J. L. (2016). Real-time monitoring of the metabolic capacity of ex vivo rat olfactory mucosa by proton transfer reaction mass spectrometry (PTR-MS). *Anal Bioanal Chem, 408*(6), 1539-1543. https://doi.org/10.1007/s00216-015-9289-7.

Thiebaud, N., Da Silva, S. V., Jakob, I., Sicard, G., Chevalier, J., Menetrier, F., . . . Le Bon, A. M. (2013). Odorant Metabolism Catalyzed by Olfactory Mucosal Enzymes Influences Peripheral Olfactory Responses in Rats. *PLoS ONE, 8*(3). https://doi.org/10.1371/journal.pone.0059547.

590 Uhlén, M., Fagerberg, L., Hallström, B. M., Lindskog, C., Oksvold, P., Mardinoglu, A., . . . Pontén, F. (2015).
591 Tissue-based map of the human proteome. *Science, 347*(6220), 1260419.
592 https://doi.org/10.1126/science.1260419.
593 Vondracek, M., Xi, Z., Larsson, P., Baker, V., Mace, K., Pfeifer, A., . . . Grafstrom, R. C. (2001). Cytochrome
594 P450 expression and related metabolism in human buccal mucosa. *Carcinogenesis, 22*(3), 481-488.
595 https://doi.org/DOI 10.1093/carcin/22.3.481.
596 Wright, K. M., Hills, B. P., Hollowood, T. A., Linforth, R. S. T., & Taylor, A. J. (2003). Persistence effects in
597 flavour release from liquids in the mouth. *International Journal of Food Science and Technology,*
598 *38*(3), 343-350. https://doi.org/10.1046/j.1365-2621.2003.00680.x.
599 Zaccone, E. J., Goldsmith, W. T., Shimko, M. J., Wells, J. R., Schwegler-Berry, D., Willard, P. A., . . . Fedan, J. S.
600 (2015). Diacetyl and 2,3-pentanedione exposure of human cultured airway epithelial cells: Ion
601 transport effects and metabolism of butter flavoring agents. *Toxicology and Applied Pharmacology,*
602 *289*(3), 542-549. https://doi.org/10.1016/j.taap.2015.10.004.
603 Zhang, L., Vlad, A., Milcarek, C., & Finn, O. J. (2013). Human mucin MUC1 RNA undergoes different types of
604 alternative splicing resulting in multiple isoforms. *Cancer Immunology, Immunotherapy, 62*(3), 423-
605 435. https://doi.org/10.1007/s00262-012-1325-2.

606

607

608 **Figure 1**

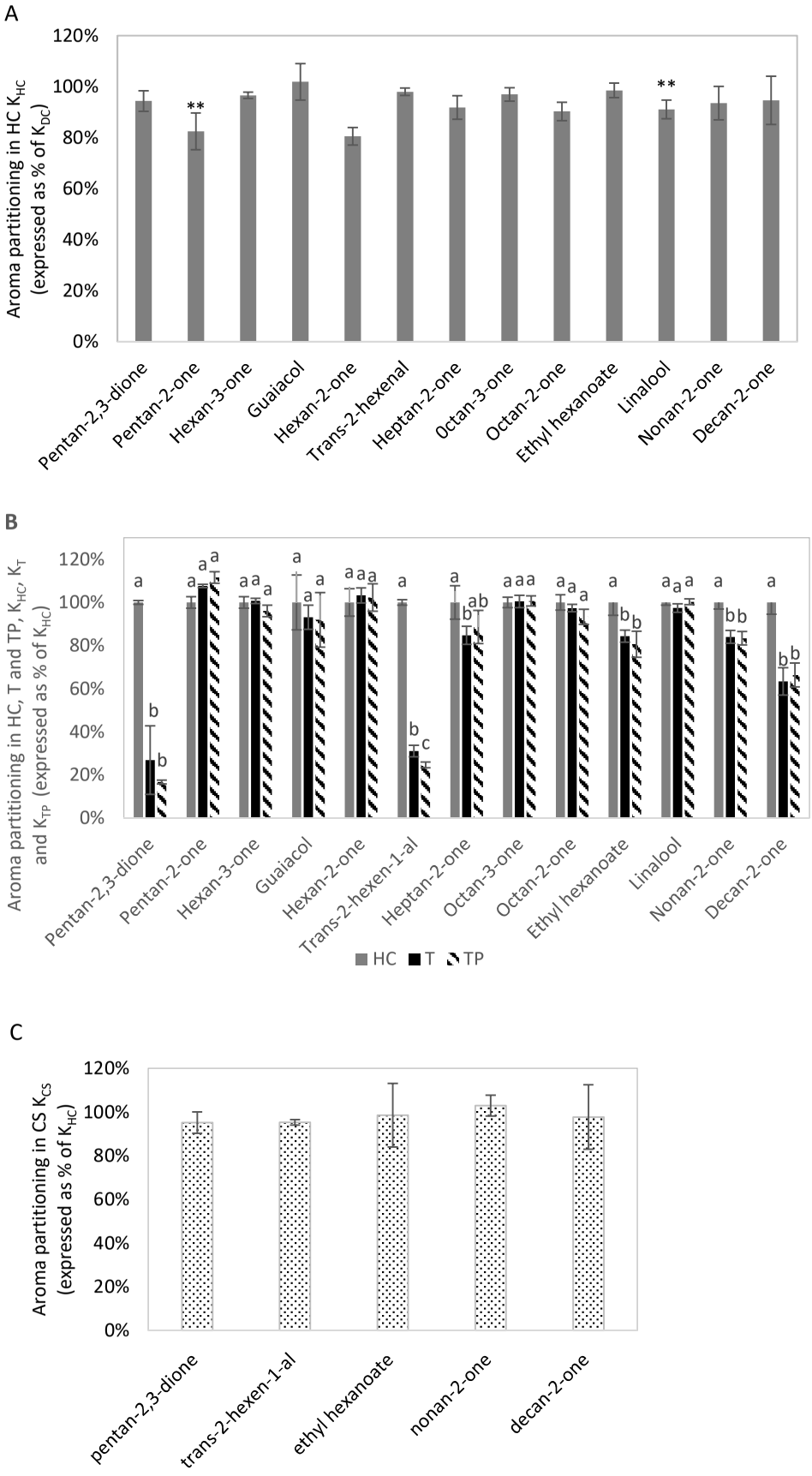

611

612

613 **Figure 2**

614

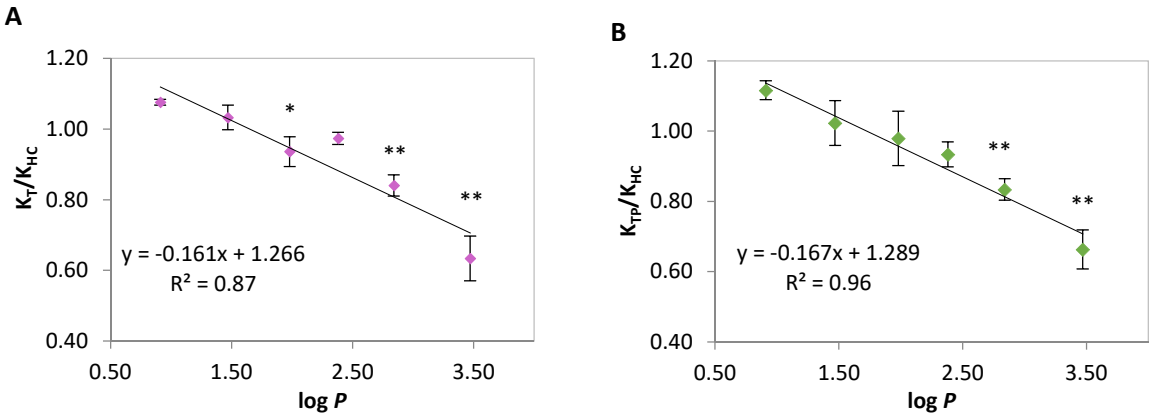

615

616

617 **Figure 3**

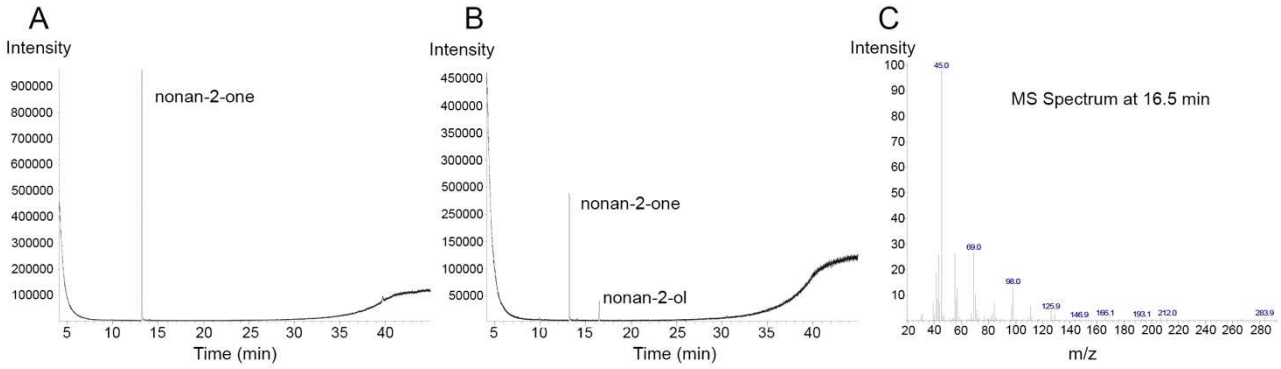

618

619

Figure 4

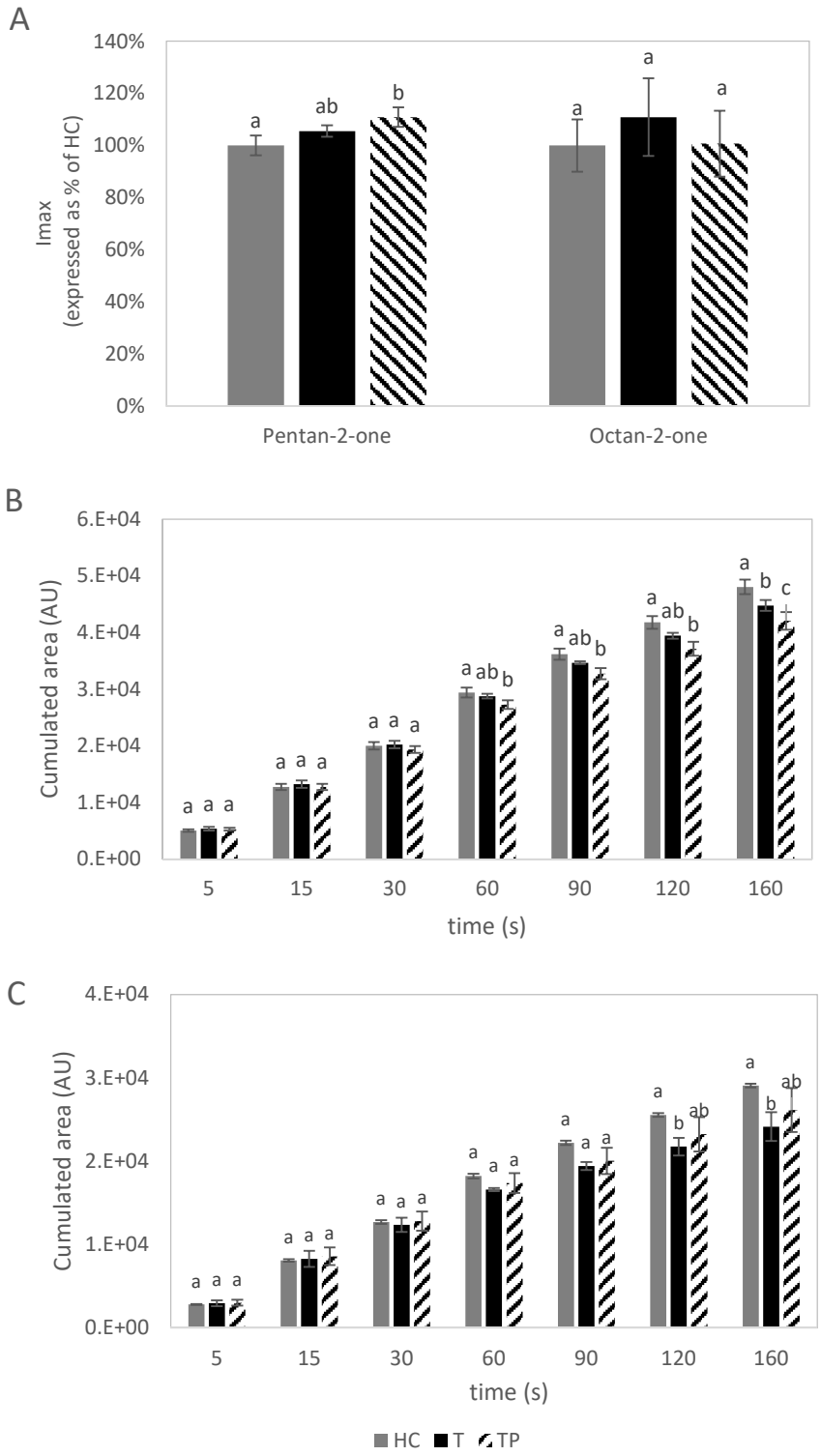
A
140%
120%
100%
80%
60%
40%
20%
0%
Imax
(expressed as % of HC)
a
ab
b
a
a
a
Pentan-2-one
Octan-2-one
B
6.E+04
5.E+04
4.E+04
3.E+04
2.E+04
1.E+04
0.E+00
Cumulated area (AU)
a a a
a a a
a a a
a ab b
a ab b
a ab b
a b c
5
15
30
60
90
120
160
time (s)
C
4.E+04
3.E+04
2.E+04
1.E+04
0.E+00
Cumulated area (AU)
a a a
a a a
a a a
a a a
a a a
a b ab
a b ab
5
15
30
60
90
120
160
time (s)
HC
T
TP

625 ***Table 1: list of compounds used in the study with their main physicochemical parameters***

Compound	CAS number	MW [a] (g/mol)	Log *P* [b]	Sol [c] (mg/l)	Pvap [d] (mmHg)	GC Oven Temp (°C)	Stock solution conc. (mg/l)	Final conc. tested for toxicity test and GC-FID-HS analyses (mg/l)
Pentan-2-one	107-87-9	86	0.91	$2.1.10^4$	39.4	70	86.0	8.6
Hexan-2-one	591-78-6	100	1.38	$7.7.10^3$	11.6	80	100.0	10
Heptan-2-one	110-43-0	114	1.98	$2.1.10^3$	3.86	95	114.0	11.4
Octan-2-one	111-13-7	128	2.37	884.2	1.35	100	128.0	12.8
Nonan-2-one	821-55-6	142	3.14	170.6	0.62	125	142.0	14.2
Decan-2-one	693-54-9	156	3.73	46.43	0.27	135	31.2	15.6
Hexan-3-one	589-38-8	100	1.24	$1.0.10^4$	13.90	80	100.0	10.0
Octan-3-one	106-68-3	128	2.22	$1.2.\ 10^3$	2.00	95	128.0	12.8
Pentan-2,3-dione	600-14-6	100	-0.85	$6.2.10^5$	31.1	80	100.0	10.0
Linalool	78-70-6	154	2.97	$1.5.10^3$	0.16	135	154.0	15.4
Guaiacol	90-05-1	124	1.32	$2.8.10^4$	0.10	Grad [e]	$1.24.10^3$	124.0
Trans-2-Hexen-1-al	6728-26-3	98	1.58	$1.6.10^4$	4.72	95	98.0	9.8
Ethyl hexanoate	123-66-0	144	2.83	629	1.8	95	144.0	14.4
Pyrazine	290-37-9	80	-0.26	$2.2.10^5$	10.8	100	800.0	80.0
2,3-dimethylpyrazine	5910-89-4	108	0.54	$3.8.10^4$	2.74	100	$1.08.10^3$	108.0

[a] Molecular weight [b] partition coefficient octanol/water Episuit [c] Solubility in water at 25 °C [d] Vapour pressure

[e] Temperature gradient for guaiacol analysis: 120°C to 150°C at 8°C/min then 150°C to 200°C at 5°C/min.

626

627

628 ***Table 2: GC-MS identification of new compounds generated after aroma exposure to the***
629 ***model mucosa and their conversion rates.*** *Conversion rates are expressed as mean value* ± SD.
630 *Different letters indicate a significant difference (Tukey test, α=0.05) between aroma compounds.*
631 *Different numbers indicate a significant difference (p< 0.05) between T and TP condition (p< 0.05).*
632

Initial aroma compounds	**New compounds identified**	**Calculated conversion rate (T) (mM/L/min)**	**Calculated conversion rate (TP) (mM/L/min)**
Pentan-2,3-dione	2-hydroxy-pentan-3-one + 3-hydroxy-pentan-2-one	1.87 ± 0.38 ^{1,a}	2.11 ± 0.02 ^{1,a}
Trans-2-hexen-1-al	Hexenoic acid	1.74 ± 0.07 ^{1,a}	1.90 ± 0.03 ^{2,a}
Ethyl hexanoate	Hexanoic acid	0.42 ± 0.07 ^{1,b}	0.51 ± 0.15 ^{1,b}
Nonan-2-one	Nonan-2-ol	0.53 ± 0.07 ^{1,bc}	0.55 ± 0.07 ^{1,bc}
Decan-2-one	Decan-2-ol	1.00 ± 0.15 ^{1,c}	0.93 ± 0.13 ^{1,c}

633

Figure captions

Figure 1: (A) Partition coefficient of aroma in hydrated control (HC) K_{HC} expressed as percentage of the value in dry control DC (K_{DC}). Mean values are reported with their standard deviation (SD). Asterisks indicate a ratio significantly lower than 100% (ANOVA, ** $p < 0.01$). **(B)** Partition coefficient of aroma after exposure to model mucosa without (K_T) and with mucosal pellicle (K_{TP}). Values are expressed as the percentage of the HC value K_{HC}. Different letters indicate significant difference between the conditions HC, T and TP (Tukey test, α=0.05). **(C)** Partitioning of aroma in clarified saliva (CS): K_{CS}. Values are expressed as the percentage of the HC value K_{HC}. All results are presented as the mean value ± SD.

Figure 2: Partition coefficient of 2-methyl ketones (K) as a function of molecules hydrophobicity (log *P*) after exposure to oral mucosa without a mucosal pellicle (K_T) **(A)** or with a mucosal pellicle (K_{TP}) **(B)**. Values are expressed as the percentage of the HC value K_{HC}. Mean values are reported with their standard deviation (SD). Asterisks indicate a ratio significantly lower than 100% (ANOVA, * $p < 0.05$, ** $p < 0.01$)

Figure 3: Data supporting the hypothesis of metabolization of nonan-2-one by oral epithelial cells. **(A)** GC-MS chromatogram of nonan-2-one extract in hydrated control (HC) **(B)** GC-MS chromatogram of supernatant extract of TR146/MUC1 cells (T) after exposure to nonan-2-one **(C)** MS spectrum at elution time of the new compound generated in T condition (t=16.5 min).

Figure 4: Effect of model mucosa without (T) or with (TP) a mucosal pellicle on dynamic release of pentan-2-one and octan-2-one. **(A)** Experimental set-up for the real-time measurements of aroma release from model mucosa **(B)** Imax = maximum aroma release intensity, CA(t) = Cumulated Area of pentan-2-one **(C)** and octan-2-one **(D)** release at different times. Results are presented as the mean value ± SD. For each parameter, different letters indicate significant difference between the conditions HC, T and TP (Tukey test, α=0.05).

Table 1: list of compounds used in the study with their main physicochemical parameters

659 **Table 2:** GC-MS identification of new compounds generated after aroma exposure to the model
660 mucosa and their conversion rates.

661 **Supplementary Material S1*:*** (a) real time monitoring of m/z ion intensity (b) curve of release of ion
662 m/z (c) curve of cumulated area under the curve.

663 **Supplementary Material S2:** GC-FID calibration curves of aroma compounds.

664 **Supplementary Material S3:** Data supporting the hypothesis of metabolization of aroma
665 compounds by oral epithelial cells. **(Left)** GC-MS chromatograms of initial compounds extract in
666 hydrated control (HC) **(Middle)** GC-MS chromatogram of supernatant extract of TR146/MUC1 cells
667 (T) after exposure to aroma solution **(Right)** MS spectra at elution time of the new compound
668 generated in T condition.

669